ISSN : 0974 - 7486 Volume 14 Issue 8

Materials Science

An Indian Journal

Full Paper

MSAIJ, 14(8), 2016 [300-306]

Synthesis and characterization of $Cu_{1-x}Co_xFe_2O_4$ nanocomposite ferrites

Nasser K.Hejazy

Al-Quds Open University, Gaza Branch, Department of Education, Gaza Strip, Gaza, (PALESTINE)

E-mail: naserkhejazy@hotmail.com

ABSTRACT

In the present study, cobalt substituted copper ferrite nanocomposite have been investigated. A series of co-doped copper ferrites with nominal compositions $Cu_{1-x}Co_xFe_2O_4$ (x = 0.0, 0.2, 0.4, 0.6, 0.8, 1.0) were synthesized by the co-precipitation oxalate rout method. The synthesized product has been characterized by powder X- ray (XRD), Transition electron microscopy (TEM), UV visible spectrophotometry, energy dispersive X-ray spectroscopy (EDX) and photoluminescence (PL). The XRD analysis reveals that the samples were cubic ferrite with average particle size in the range 12.1- 13.5 nm. The micrographs obtained from TEM analysis showed that the synthesized materials have a spherical shape with an agglomeration of the individual particles. The energy dispersive X-ray spectrometric analysis revealed that the observed molar ratios of different components of the samples are in close agreement with their nominal compositions. The optical band gap values for pure copper ferrite and doped copper ferrite nanoparticles was found to be 3.72 -3.03 eV, respectively. PL spectra of pure copper ferrite and doped copper ferrite nanoparticles showed blue emission at 460 nm and green emission at 520 nm.

KEYWORDS

Characterization;
Nanocomposite;
Synthesis;
Ferrites.

INTRODUCTION

Spinel ferrites with a general composition MFe_2O_4 ($M=Co^{2+}, Cu^{2+}$) exhibit interesting magnetic, magneto-resistive and magneto-optical properties. At the same time, these compounds have well-established catalytic properties for many reactions such as oxidative dehydrogenation of hydrocarbons, decomposition of alcohols, selective oxidation of carbon monoxide, decomposition of hydrogen peroxide, and hydrodesulphurization of petroleum crude[1]. The catalytic properties of ferrospinels crucially depend on the distribution of cations among the octahedral and tetrahedral sites of the spinel structure. Jacobs et al.[2] established that, in spinels, the octahedral sites are almost exclusively exposed in the crystallites and that the catalytic activity was mainly due to cations located in octahedral sites. Cobalt ferrite ($CoFe_2O_4$) is a well-known hard ferrite material, which has been studied in detail due to its high coercivity and moderate saturation magnetization[3]. Copper ferrite ($CuFe_2O_4$) is mostly an inverse spinel structure[4]. Various research groups have studied the effect of doping with different cations to enhance physical properties of spinel ferrites[5]. Gautam et al[6] reported electronic structure studies of Cu^{2+} doped cobalt ferrite, they observed that Cu^{2+} ions

occupy octahedral site.

Many techniques have been used for the determination of cation distribution by using the X-ray diffraction such as R-factor[7,8], Furuhashi[9] and Bertaut methods[10]. The additional techniques include neutron diffraction[11], thermoelectric measurements[12], and electron spin resonance[13]. The intensity of X-ray reflections reveals a reliance on the possession of cations amongst the interstitial sites. So all of the above said methods in which X-ray diffraction has been used, are based upon the comparison of experimentally observed intensities with those, calculated for the hypothetical crystal structure[14]. Cobalt ferrite is reported as an inverse spinel and the degree of inversion is strongly dependent on the preparation conditions and methods[15,16]. The distribution of cations in copper ferrites, prepared by co-precipitation technique is reported as $[Cu_{0.2}Fe_{0.8}]\,[Cu_{0.8}Fe_{1.2}]\,O_4$. Although a lot of work has been done on $CoFe_2O_4$ and $CuFe_2O_4$, a little work is found in literature on mixed Co–Cu ferrites. Tailhades et al.[17] prepared mixed cobalt–copper spinel ferrites $Co_xCu_{1-x}Fe_2O_4$ with a cicular shape from oxalate precursors and reported that the cation distribution is sensitive to the thermal history of the samples.

This paper reports the effect of Co-doping on structural, morphological and optical of $CuFe_2O_4$ (x=0.0,0.2,0.4,0.6,0.8,1.0) nanocomposites prepared by the co-precipitation oxalate rout chemical method. The present investigation is concerned with the synthesis of copper ferrite magnetic nanoparticles with controlled particle size, particle size distribution, composition and surface morphology. Various characterization techniques have been carried out using X-ray diffraction (XRD), transmission electron microscopy (TEM), energy dispersive X-ray spectroscopy (EDX), UV–visible spectroscopy and PL spectroscopy.

EXPERIMENTAL

All reagents used in the present work were analytical grade and directly used without further treatment. Oxalic acid, $H_2C_2O_4.2H_2O$ (Merck, 99.5% purity), Praepagen HY, $C_{16}H_{36}NOCl$ (Clariant, 40%), Zinc sulfate monohydrate, $ZnSO_4.H_2O$ (Merck, 99% purity), Copper sulfate pentahydrate, $CuSO_4.5H_2O$ (Merck, 99% purity), Ferrous ammonium sulfate hexahydrate, $(NH_4)_2Fe(SO_4)_2.6H_2O$ (Merck, 99.5% purity) and deionized water were used in the synthesis and preparation of all solutions. In typical synthesis of $Cu_{1-x}Co_xFe_2O_4$ with x= (0.0, 0.2, 0.4, 0.6, 0.8,1) nanopowders, (20 mmol) of Ferrous ammonium sulfate and the respective amounts Copper sulfate and doped metal ions of Co were dissolved into 25 mL of deionized water. (20 mmol) of oxalic acid was dissolved in an equal volume of deionized water and dropwise added to metal salts solution under magnetic stirring for 60 min, a precipitate of (Cu, Co, Fe) oxalate was isolated, washed with water several times and dried at 100°C for 24 hours. The dried material was grounded using mortar and pestle to produce fine powder precursor. Subsequently, the precursor, (Cu, Co, Fe) oxalate was annealed in muffle furnace under air at 500°C for 3 h to form $Cu_{1-x}Co_xFe_2O_4$ nanostructure.

UV–vis absorption spectra were collected using a UV–vis spectrophotometer (Shimadzu, UV-2400) in the wavelength range from 200 to 700 nm. PL spectra were recorded with a spectrofluorometer (JASCO, FP-6500); the extinction wavelength was selected to be 400 nm. The X-ray diffraction (XRD) patterns of the dried as-prepared and classified samples were obtained using an X-ray diffractometer PANalytical X´pert (PANalytical) with Cu Ka radiation (0.154 nm wavelength) under 40 kV and 200 mA. The transmission electron microscopy (TEM) analysis was done with JEM2010 (JEOL) transmission electron microscope with eenergy dispersive X-Ray Spectrometer INCA (Oxford Instruments).

RESULTS AND DISCUSSION

The structure and phase purity of the samples were confirmed by analyzing the X-ray powder diffraction patterns. Figure 1 shows the XRD patterns of $Cu_{1-x}Co_xFe_2O_4$ samples prepared at various Co substitutions x = (0.0, 0.2, 0.4,0.6, 0.8 and 1.0). All the observed reflections could be assigned to cubic spinel lattice indicating their single phase structure with some traces of other impurity phases (e.g. Fe_2O_3 and CuO phases). The peaks could be indexed as (220), (311), (222), (400), (422), (511), and (440), which are characteristics of single-phase cubic spinel structure (JCPDS card no. 22-1012). From the results, the Cu-Co ferrite phase

Full Paper

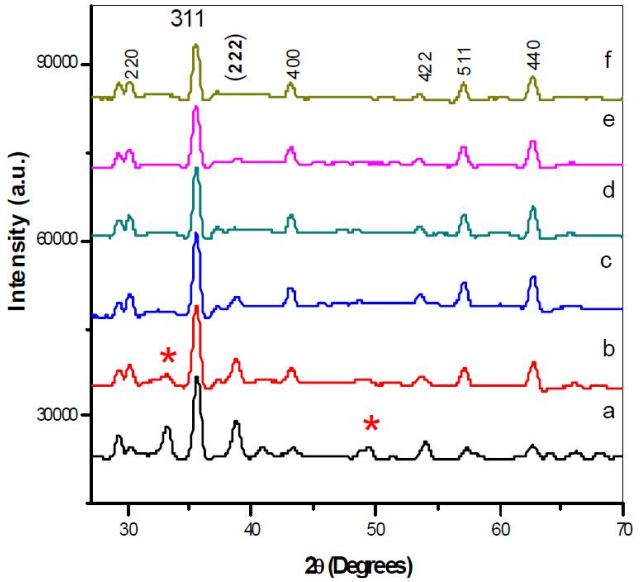

Figure 1 : XRD 0f (a) $Cu_{0.005}Fe_2O_4$, (b) $Cu_{0.004}Co_{0.001}Fe_2O_4$, (c) $Cu_{0.003}Co_{0.002}Fe_2O_4$, (d) $Cu_{0.002}Co_{0.003}Fe_2O_4$, (e) $Cu_{0.001}Co_{0.004}Fe_2O_4$, (f) $Co_{0.004}Fe_2O_4$

formed contained some impurity peaks, which are due to decomposition of the ferrites to α-Fe_2O_3 phase, above the annealing temperature of 500°C[18–20]. The intensity of main diffraction peak of cubic spinel ferrite at the (311) plane was considered as a measure of its degree of crystallinity[21]. An increase in the concentration of Co in copper ferrite resulted in a measurable progressive increase in the degree of crystallinity of the produced cubic phase. The average particle sizes of the samples were estimated from the broadening of the diffraction peaks using the Debye–Scherrer equation. The average particle size of all samples in the range of 12.1-13.5 nm. It was found that by increasing the amount of cobalt loading, the crystallite size increases. It is may be due to the surface temperature that affects the molecular concentration and makes the tiny crystal to grow at the surface of the crystal, thereby increasing the molecular concentration at the crystal surface, which in turn increases the grain growth[22].

The morphological characteristics of the obtained $Cu_{1-x}Co_xFe_2O_4$ (x=0.0,0.6,0.8,1.0) nanoparticles were investigated by the transmission scanning electron microscopy (TEM) and are shown in Figure 2(a-c). The figures proved that products are nearly cubic (not uniform) with diameter 32-40 nm as calculated from histogram (see Figure 2). Nanoparticles are agglomerated due to the presence of magnetic interactions among the particles[23]. The observed difference in particle size calculated by XRD and as observed by TEM may be due to the molecular structural disorder and lattice strain, which resulted the different ionic radii and/or clustering of the nanoparticles.

EDX spectroscopy is an analytical tool to determine the composition of the sample. EDX spectra of $Cu_{1-x}Co_xFe_2O_4$ ferrites (x = 0.0, 0.6, 0.8, 1) are shown in Figure 3(a-c). Figure 3 shows the peaks of Fe, Cu and O elements in pure. It is interesting to note that the preparation condition completely favors the formation of mixed ferrites and allow us to study the effect of increasing Co content on the properties of the copper ferrite. The above mentioned results confirm the formation of pure and Co-doped $CuFe_2O_4$ phase.

UV-vis spectral analysis has been widely used to characterize semiconductor nanoparticles. As the particle size decreases, the absorption edge shifts to shorter wavelength, due to the band gap increase of the smaller particles [108, 109]. The absorption spectra of Cu ferrite and Co doped in Cu ferrite nanoparticles ($Cu_{1-x}Co_xFe_2O_4$) in UV-light region was illustrated in Figure 4. It can be clearly seen that all samples possessed an absorption band in the whole range as well as exhibited a good absorption in the light region (330-400 nm). The absorption at 330 nm is assigned to the characteristic absorption band of $CuFe_2O_4$ nanoparticles. On substituting Co in copper ferrites, the absorption band is shifted to longer wavelength as shown in Figure 4. The fundamental absorption, which corresponds to electron excitation from the valance band to conduction band, can be used to determine the value of the optical band gap of the synthesized $Cu_{1-x}Co_xFe_2O_4$ ferrite nanoparticles. The band gap can be obtained from a linear extrapolation of the absorbance edge to the wavelength axis. The estimated band gap values of $Cu_{1-x}Co_xFe_2O_4$ (x = 0.0, 0.2, 0.4, 0.6, 0.8 and1.0) nanostructures was found to be 3.72 -3.03 eV (see Figure 5). The band gap energy decreases with increasing Co content, which may be associated with various parameters including the crystallite size, structural parameter, carrier concentrations, presence of very small amount of impurities which are detectable by XRD technique and lattice strain[24].

In order to study the defects and other impurity states of the system, photoluminescence (PL) spectra of the Co-doped $CuFe_2O_4$ samples were recorded.

Figure 6 shows room temperature PL spectrum of $Cu_{1-x}Co_xFe_2O_4$ where x = (0.0, 0. 2, 0. 4, 0. 6, 0. 8 and 1.0). The excitation was recorded at wavelength 400 nm. All the samples showed the characteristic near-band-edge (NBE) emission of pure and Co-doped $CuFe_2O_4$ at around 460 nm. A broader visible emission band was obtained for all the samples centered at 460 nm, and is attributed to the recombination of electrons

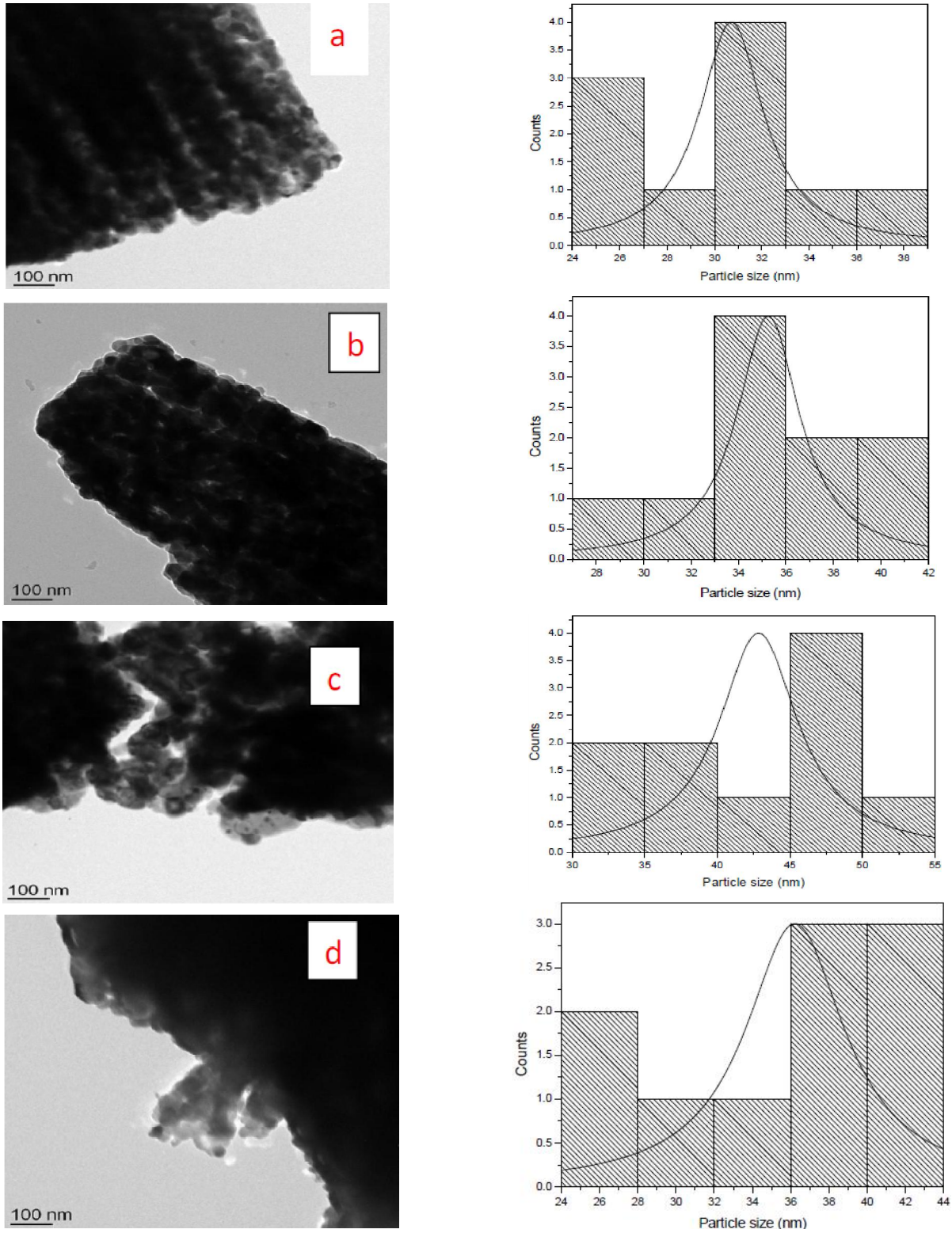

Figure 2 : TEM micrographs and EDX spectrum of of $Cu_{1-x}Mn_xFe_2O_4$ (a) x=0.0, (b) x=0.2, (c) x=0.8 and (d) x=1.

Full Paper

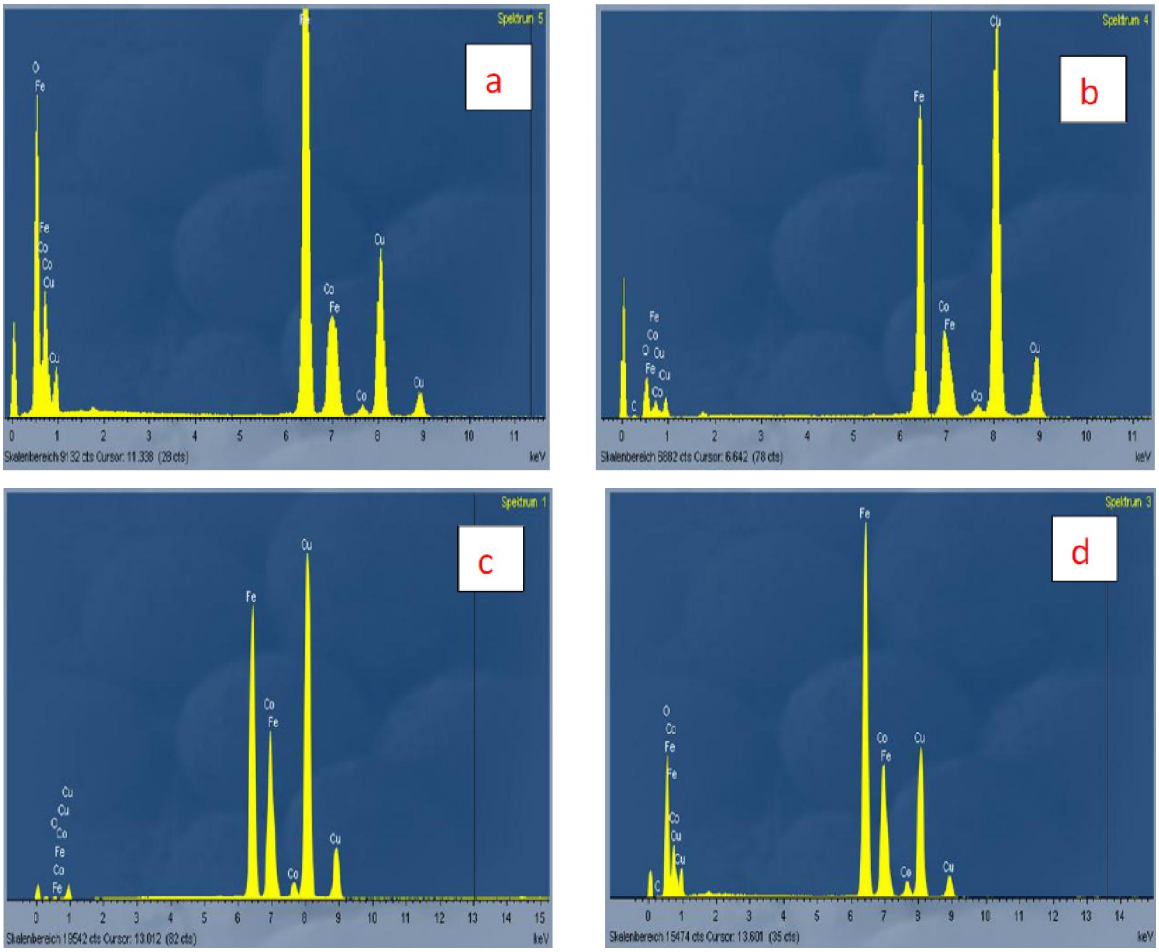

Figure 3 : EDX spectrum of $Cu_{1-x}Co_xFe_2O_4$ (a) x=0.0, (b) x=0.6, (c)x=0.8 and (d) x=1.

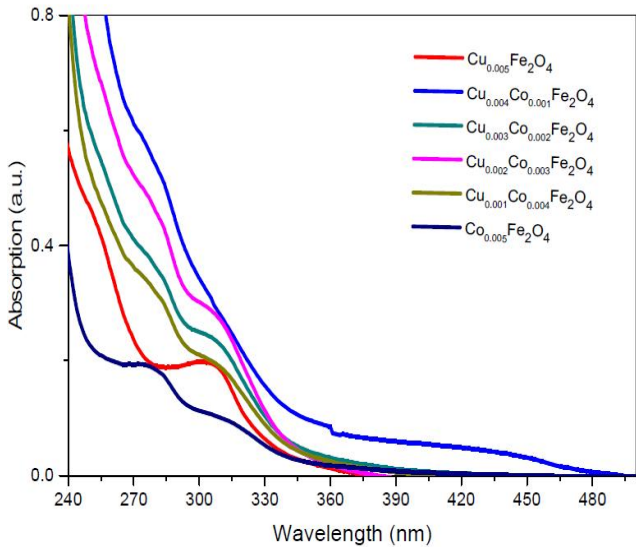

Figure 4 : UV-vis. spectra of $Cu_{1-x}Co_xFe_2O_4$ x = (0.0, 0.2, 0.4, 0.6, 0.8 and 1.0)

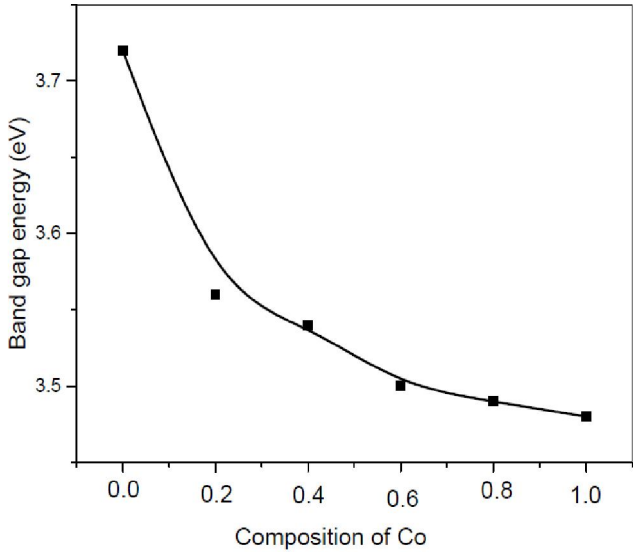

Figure 5 : Variation of the band gap energy of $Cu_{1-x}Ni_xFe_2O_4$ (x = 0.0, 0.2, 0.4, 0.6, 0.8 and 1.0)

deeply trapped in oxygen vacancies with photo generated holes[25]. As we increase the doping concentration of Co into $CuFe_2O_4$, overall intensities of the peak for all the samples decrease. This behavior can be attributed to the appearance of new electronic levels between the conduction and the valence band

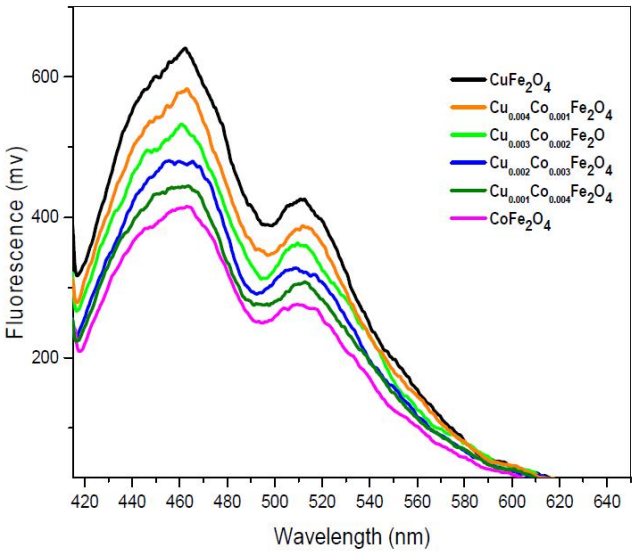

Figure 6 : Photoluminescence spectra of $Cu_{1-x}Co_xFe_2O_4$ ferrite at x= (0.0 ,0.2 ,0.4 ,0.6 ,0.8 ,1.0)

and might be due to the increase in intrinsic defects[26].

CONCLUSION

Copper ferrite nanoparticles doped with transition metal (Co) were successively synthesized by a co-precipitation chemical method. The crystalline structure of $Cu_{1-x}Co_xFe_2O_4$ was investigated by X-ray diffraction, which confirms that $Cu_{1-x}Co_xFe_2O_4$ ferrites have a cubic spinel structure as matched with JCPDS card. It is observed that the crystallite size of nano ferrites is found to be increased with increasing doping content. The obtained TEM images showed that the synthesized materials have a spherical shape with an agglomeration of the individual particles.

The optical band gap values for pure copper ferrite and doped copper ferrite nanoparticles was found to be 3.72 -3.03 eV, respectively. PL spectra of pure copper ferrite and doped copper ferrite nanoparticles showed blue emission at 460 nm and green emission at 520 nm.

REFERENCES

[1] C.G.Ramankutty, S.Sugunan; Applied Catalysis A, **218**, 39–51 **(2001)**.

[2] J.P.Jacobs, A.Maltha, J.G.H.Reintjes, J.Drimal, V.Ponec, H.H.Brongersma; Journal of Catalysis, **147**, 294 **(1994)**.

[3] Y.Pu et al.; Materials Research Bulletin, **45**, 616–620 **(2010)**.

[4] S.Y.An et al.; Thin Solid Films, **519**, 8296–8298 **(2011)**.

[5] P.P.Hankare et al.; Materials Letters, **61**, 2769–2771 **(2007)**.

[6] S.Gautam, S.Muthurani, M.Balaji, P.Thakur; Journal of Nanotechnology, **11**, 386 **(2011)**.

[7] P.K.Baltzer, P.J.Wojtowicz, M.Robbins, E.Lopatin; Physical Review, **151**, 367 **(1966)**.

[8] A.Hussain,T.Abbas, S.B.Naizi; Ceramics International, **07**, 049S **(2012)**.

[9] H.Furuhashi, M.Inagaki, S.Naka; Journal of Inorganic and Nuclear Chemistry, **35**, 3009–3014 **(1973)**.

[10] J.M.Rubio Gonzalez, C.O.Arean; Journal of the Chemical Society, Dalton Transactions, 2155–2159, **(1985)**.

[11] E.Stoll, P.Fischer, W.Halg, G.Maier; Journal de Physique Paris, **25**, 447–448 **(1964)**.

[12] C.C.Wu, T.O.Mason; Journal of the American Ceramic Society, **64**, 520–522 **(1981)**.

[13] U.Schmocker, H.R.Boesch, F.Waldner; Physics Letters A, **40**, 237–238 **(1972)**.

[14] Q.Wei, J.Li, Y.Chen,Y.Han; Materials Characterization, **47**, 247–252 **(2001)**.

[15] D.R.Mane, U.N.Devatwal, K.M.Jadhav; Materials Letters, **44**, 91–95 **(2000)**.

[16] C.Nlebedim, N.Ranvah, P. I.Williams, Y.Melikhov, F.Anayi, J.E.Synder, A.J.Moses, D.C.Jiles; Journal of Magnetism and Magnetic Materials, **321**, 2528–2532 **(2009)**.

[17] Ph.Tailhades, C.Villette, A.Rousset, G.U.Kulkarni, K.R.Kannan; Journal of Solid State Chemistry, **141**, 56–63 **(1998)**.

[18] Pan, H.Wang, J.-j.Tian, S.-g.Zhang, X.-f.Wang, Alex A.Volinsky; J. Magn. Magn. Mater, **322**, 173 **(2010)**.

[19] R.Abolhassani, S.Manouchehri, M.H.Keshavarz, S.Fatahian; J. Magn. Magn. Mater, **323**, 730 **(2011)**.

[20] N.M.Deraz, A.Alarifi; J.Anal, J.Appl.Pyrol., **94**, 41 **(2012)**.

[21] A.Navrotsky, O.J.Kleppa; J.Inorg.and Nucl. Chem., **30**, 479 **(1968)**.

[22] M.A.Rehman, M.Mumatz, S.Naeem, I.L.Papst; J. Ceram.Int., **39**, 5235 **(2013)**.

[23] G.C.David, K.F.Wayne, E.G.Kenneth, D.M.Gerald, M.Arun; Humphrey, J. Applied Physics, **93**, 793 **(2003)**.

[24] L.Deyu, W.Yiying, K.Philip, S.Li, Y.Peidong,

M.Arun; J.Appl.Physi. Lett., 2934 **(2003)**.

[25] R.B.Kale, C.D.Lokhande; J.Appl.Surf.Sci., **223**, 343 **(2004)**.

[26] A.V.Dijken, E.A.Meulenkamp, D.Vanmaekelbergh, A.Meijerink; J.Lumin., **90**, 123 **(2000)**.

[27] A.Manikandan, J.Judith Vijaya, L.John Kennedy, M.Bououdina; J. Mole.Stru., **1035**, 332 **(2013)**.